

Carbon Radical Generation by d^0 Tantalum Complexes with α -Diimine Ligands through Ligand-Centered Redox Processes

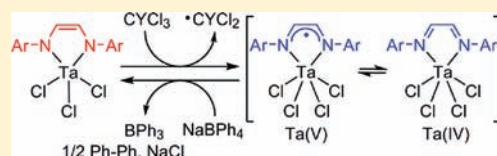
Hayato Tsurugi,[†] Teruhiko Saito,[†] Hiromasa Tanahashi,[†] John Arnold,[‡] and Kazushi Mashima^{*,†}

[†]Department of Chemistry, Graduate School of Engineering Science, Osaka University, Toyonaka, Osaka 560-8531, Japan

[‡]Department of Chemistry, University of California, Berkeley, California 94720, United States

S Supporting Information

ABSTRACT: High-valent tantalum complexes having redox-active α -diimine ligands, (α -diimine)TaCl_{*n*} (*n* = 3, 4), are prepared by the reaction of TaCl₅, α -diimine ligands, and an organosilicon-based reductant, 1-methyl-3,6-bis(trimethylsilyl)-1,4-cyclohexadiene. Reductive cleavage of the C–Cl bond of polyhaloalkanes is accomplished by trichlorotantalum complexes having dianionic α -diimine ligands via electron transfer from the dianionic ligands, whereas oxidative decomposition of tetraphenylborate is observed using tetrachlorotantalum complexes with monoanionic α -diimine ligands through electron transfer to the monoanionic ligands. Chemically oxidized or reduced complexes of (α -diimine)TaCl₄ are isolated as ligand-centered redox products, [Cp₂Co][(α -diimine)TaCl₄] and [(α -diimine)TaCl₄][WCl₆], where the α -diimine ligand coordinates to the metal center as a dianionic or neutral ligand, respectively. On the basis of EPR measurements of (α -diimine)TaCl₄ complexes (which are key intermediates for reductive cleavage of C–Cl bond and oxidative decomposition of tetraphenylborate), two redox isomers—a tantalum-centered radical and ligand-localized radical—are present in solution.

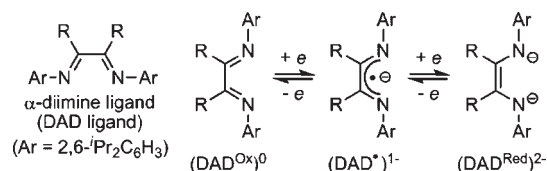


INTRODUCTION

Transition metal complexes may mediate bond formation and bond cleavage by utilizing redox processes. One-electron redox processes at a metal center are considered to be radical reactions, whereas oxidative addition and reductive elimination reactions are events accompanied by two electron redox at the metal.¹ In addition, ligand-centered redox processes have attracted much interest as alternatives to metal-centered redox cycles because of increased flexibility on designing catalysts.^{2–6} Recent progress for utilizing redox-active metal and ligand combination, such as bis(imino)pyridine iron(II)³ and bis(aminophenolate) cobalt(II)⁴ complexes, enable us to use first-row transition metals as catalysts for carbon–carbon bond-forming reactions. In some instances, it has been shown that ligand-localized π -radical species are involved as key intermediates. Furthermore, several research groups have focused on electrophilic d^0 early transition metal complexes supported by redox-active ligands, and oxidative addition of halogens and dioxygen and reductive elimination from dialkyl species are possible through formation of open-shell ligand π -radical species as intermediates.^{6d,k} Because of the stability of high oxidation states of early transition metals, it is possible to study purely ligand-based redox events and the character of open-shell ligand π -radicals using d^0 -metal complexes.⁶

The 1,4-diaza-1,3-butadiene (α -diimine) class of ligands are important in this regard because of (i) their flexibility on tuning the coordination modes suitable to transition metals and (ii) their one-electron or two-electron reductions, producing π -radical monoanions and ene-diamide dianions, respectively (Chart 1).^{5h,k,l,o,7,8} Based on the redox reactivity of the α -diimine

Chart 1. Three Electronic Structures of α -Diimine Ligands



ligands, Abu-Omar et al. reported a multielectron transfer process from the α -diimine ligands to dioxygen on the central metal leading to η^2 -peroxo formation for (α -diimine)₂Zr complexes.^{6b} In addition, (α -diimine)MCl_{*x*} complexes were anticipated to be an interesting platform to investigate ligand-based valence changes in d^0 early transition metal complexes. However, the preparation of (α -diimine)MCl_{*x*} via simple salt metathesis reactions has been problematic, with intractable mixtures hampering the isolation of desired products.⁹ These results impeded precise evaluation of the role of α -diimine ligands during the redox reaction.

We recently reported that 1-methyl-3,6-bis(trimethylsilyl)-1,4-cyclohexadiene (MBTCD) acted as a unique reducing reagent for early transition metal halides, such as NbCl₅ and TaCl₅, to give low valent species without any salt contamination.¹⁰ In situ generated low-valent species reacted smoothly with redox-active

Received: May 21, 2011

Published: October 07, 2011

α -diimine ligands to form (α -diimine)TaCl_x complexes. Herein we report the reductive cleavage of the carbon–halogen bond of polyhaloalkanes through electron transfer from the dianionic α -diimine ligands to polyhaloalkanes. The generated radicals add to the α -diimine ligand backbone or styrene to form new C–C bonds. Oxidative decomposition of tetraphenylborate proceeds via transfer of one electron from the borate anion to the mono-anionic α -diimine ligand. To the best of our knowledge, this is the first example of controlled radical generation from polyhaloalkanes and organoborate via redox reactions using d⁰ metal complexes with redox active ligands. Furthermore, tantalum complexes having open-shell ligand π -radicals are fully characterized by EPR measurements and X-ray diffraction studies.

EXPERIMENTAL SECTION

General. All manipulations involving air- and moisture-sensitive organometallic compounds were carried out under argon using standard Schlenk techniques or in an argon-filled glovebox. 1-Methyl-3,6-bis-(trimethylsilyl)-1,4-cyclohexadiene (MBTCD)¹¹ and α -diimine ligands (**1a**–**1c**)¹² were prepared according to literature procedures. Cp₂Co, and WCl₆ were purchased and used as received. Anhydrous hexane, toluene, THF, and dichloromethane were purchased from Kanto Chemical and further purified by passage through activated alumina under positive argon pressure as described by Grubbs et al.¹³ Benzene-*d*₆, toluene-*d*₈, and bromobenzene-*d*₅ were distilled from CaH₂ and degassed before use. ¹H NMR (300 MHz, 400 MHz) and ¹³C NMR (75 MHz, 100 MHz) spectra were measured on Varian UNITY INOVA-300 and Bruker AVANCEIII-400 spectrometers. Assignments for ¹H and ¹³C NMR peaks for some of the complexes were aided by 2D ¹H–¹H COSY, 2D ¹H–¹³C HMQC, and 2D ¹H–¹³C HMBC spectra. The EPR spectrum was recorded at 298 K on a Bruker EMX-10/12 spectrometer in toluene, CH₂Cl₂, and THF. Cyclic voltammograms were recorded in a glovebox at room temperature in CH₂Cl₂ solution containing 0.1 M [ⁿBu₄N][PF₆] or 0.1 M [ⁿBu₄N][BF₄] as the supporting electrolyte. GC–MS measurement was carried out using a DB-1 capillary column (0.25 mm × 30 m) on a Shimadzu GCMS-QP2010Plus. IR spectra were recorded on a JASCO FT/IR-230 spectrometer. All melting points were measured in sealed tubes under argon atmosphere. Elemental analyses were recorded by using Perkin-Elmer 2400 at the Faculty of Engineering Science, Osaka University.

Synthesis of (α -Diimine)TaCl₃ (2b**).** A solution of **1b** (2.9 g, 7.8 mmol) in toluene (10 mL) was added to a solution of TaCl₅ (2.8 g, 7.8 mmol) in toluene (50 mL) at room temperature. The color of the solution changed to deep red. After the mixture was stirred for 10 min, 1-methyl-3,6-bis(trimethylsilyl)-1,4-cyclohexadiene (2.0 mL, 8.4 mmol) was added. The reaction mixture was stirred for 12 h, and then all volatiles were removed under reduced pressure to give brown solid. The solid was washed with hexane (3 × 10 mL). The remaining solid was dried to give yellow powder of **2b** in 92% yield (4.8 g, 7.2 mmol), mp 210–214 °C (dec). ¹H NMR (400 MHz, C₆D₆, 308 K) δ 1.13 (d, *J* = 6.8 Hz, 12H, CH(CH₃)₂), 1.31 (d, *J* = 6.8 Hz, 12H, CH(CH₃)₂), 2.99 (sept, *J* = 6.8 Hz, 4H, CH(CH₃)), 5.67 (s, 2H, HC=CH), 7.10–7.15 (m, 6H, aromatic protons). ¹³C NMR (100 MHz, C₆D₆, 308 K) δ 24.4 (CH(CH₃)₂), 24.7 (CH(CH₃)₂), 28.8 (CH(CH₃)₂), 104.8 (HC=CH), 124.3 (*m*-Ar), 129.0 (*p*-Ar), 144.3 (*o*-Ar), 145.9 (*ipso*-Ar). Anal. Calcd for C₂₆H₃₆Cl₃N₂Ta: C, 47.04; H, 5.47; N, 4.22. Found: C, 46.76; H, 5.69; N, 4.14. UV–vis (toluene) λ_{\max}/nm ($\epsilon/\text{M}^{-1}\text{cm}^{-1}$): 403 (1.33 × 10³).

Complex **2a** was prepared in similar manner as **2b**. An orange powder was obtained in 86% yield, mp 170–171 °C (dec). ¹H NMR (400 MHz, C₆D₅Br, 308 K) δ 1.46 (d, *J* = 6.8 Hz, 12H, CH(CH₃)₂), 1.61 (d, *J* = 6.8 Hz, 12H, CH(CH₃)₂), 2.45 (s, 4H, NC(CH₃)), 3.24 (sept, *J* = 6.8 Hz, 4H, CH(CH₃)₂), 7.35–7.5 (m, 6H, aromatic protons). ¹³C NMR (100

MHz, C₆D₅Br, 308 K) δ 14.2 (NC(CH₃), 23.9 (CH(CH₃)₂), 24.3 (CH(CH₃)₂), 28.1 (CH(CH₃)₂), 110.0 (CH₃C=CCH₃), 123.7 (Ar), 127.7 (Ar), 142.0 (Ar), 145.0 (Ar). Anal. Calcd for C₂₈H₄₀Cl₃N₂Ta: C, 48.60; H, 5.83; N, 4.05. Found: C, 48.68; H, 6.04; N, 3.75.

Synthesis of [(α -Diimine)TaCl]₂(μ -Cl)₃][TaCl₆] (3c**).** A toluene (20 mL) solution of 1-methyl-3,6-bis(trimethylsilyl)-1,4-cyclohexadiene (0.17 mL, 0.72 mmol) and **1c** (0.36 g, 0.72 mmol) was added to TaCl₅ (0.38 g, 1.1 mmol) in toluene (50 mL) at room temperature. The color of the solution changed to brown. The reaction mixture was stirred for 16 h, and then all volatiles were removed under reduced pressure. The solid was washed with hexane (3 × 10 mL) and then dried under vacuum to give **3c** as a brown powder in 84% yield (0.63 g, 0.30 mmol), mp 287–289 °C (dec). ¹H NMR (400 MHz, C₆D₅Br, 308 K) δ 0.90 (d, *J* = 6.8 Hz, 12H, CH(CH₃)₂), 0.94 (d, *J* = 6.8 Hz, 12H, CH(CH₃)₂), 1.49 (d, *J* = 6.8 Hz, 12H, CH(CH₃)₂), 1.52 (d, *J* = 6.8 Hz, 12H, CH(CH₃)₂), 2.46 (m, *J* = 6.9 Hz, 4H, CH(CH₃)₂), 4.08 (m, *J* = 6.6 Hz, 4H, CH(CH₃)₂), 7.16 (d, *J* = 7.8 Hz, 4H, 3-H of acenaphthylene), 7.52 (t, *J* = 4.3 Hz, 4H, *p*-NAr), 7.54 (t, *J* = 7.8 Hz, 4H, 4-H of acenaphthylene), 7.73 (d, *J* = 4.3 Hz, 8H, *m*-NAr), 7.83 (d, *J* = 7.8 Hz, 4H, 5-H of acenaphthylene). ¹³C NMR (100 MHz, C₆D₅Br, 308 K) δ 23.4 (CH(CH₃)₂), 23.9 (CH(CH₃)₂), 24.2 (CH(CH₃)₂), 25.8 (CH(CH₃)₂), 28.1 (CH(CH₃)₂), 28.5 (CH(CH₃)₂), 109.1 (N–C=C–N), 124.8₅ (*p*-NAr), 124.8₉ (*m*-NAr), 126.9 (acenaphthylene), 127.7 (acenaphthylene), 128.1 (acenaphthylene), 130.0 (*m*-NAr), 130.4 (acenaphthylene), 140.0 (*ipso*-NAr), 141.8 (acenaphthylene), 144.3 (*o*-NAr), 144.6 (*o*-NAr). Anal. Calcd for C₇₄H₈₄Cl₁₅N₄Ta₃-(CH₂Cl₂)₂: C, 42.24; H, 4.02; N, 2.66; Found: C, 41.88; H, 4.00; N, 2.67. UV–vis (CH₂Cl₂) λ_{\max}/nm ($\epsilon/\text{M}^{-1}\text{cm}^{-1}$): 331 (2.25 × 10⁴).

Synthesis of (Enamido-imino)TaCl₄ (4a**).** Carbon tetrachloride (31.7 μ L, 0.32 mmol) was added to a solution of complex **2a** (226 mg, 0.32 mmol) in toluene (50 mL) at room temperature. The reaction mixture was stirred for 4 h at 60 °C, and then all volatiles were removed under reduced pressure to give yellow solid. The solid was washed with hexane (3 × 10 mL) and dried to give **4a** as a yellow powder in 89% yield (199 mg, 0.28 mmol), mp 199–203 °C (dec). ¹H NMR (400 MHz, C₆D₅Br, 308 K) δ 1.46 (d, *J* = 6.6 Hz, 6H, CH(CH₃)₂), 1.55 (d, *J* = 6.6 Hz, 6H, CH(CH₃)₂), 1.89 (d, *J* = 6.6 Hz, 6H, CH(CH₃)₂), 1.94 (d, *J* = 6.6 Hz, 6H, CH(CH₃)₂), 2.34 (s, 3H, NC(CH₃)C), 3.71 (sept, *J* = 6.6 Hz, 2H, CH(CH₃)₂), 3.13 (sept, *J* = 6.6 Hz, 2H, CH(CH₃)₂), 4.62 (br d, 1H, NC=CH₂), 5.33 (br d, 1H, NC=CH₂), 7.5–7.8 (m, 6H, aromatic protons). ¹³C NMR (100 MHz, C₆D₅Br, 308 K) δ 19.1 (N=CCH₃), 24.5 (CH(CH₃)₂), 24.5 (CH(CH₃)₂), 24.6 (CH(CH₃)₂), 26.2 (CH(CH₃)₂), 28.1(CH(CH₃)₂), 28.5 (CH(CH₃)₂), 114.9 (NC=CH₂), 124.2 (*m*-Ar), 125.2 (*m*-Ar), 127.7 (Ar), 128.3 (Ar), 129.5 (Ar), 140.2 (*o*-Ar), 144.3 (Ar), 145.2 (*o*-Ar), 153.1 (NC=CH₂), 182.0 (C=N). Anal. Calcd for C₂₈H₃₉Cl₄N₂Ta(CH₂Cl₂): C, 42.93; H, 5.09; N, 3.45. Found: C, 43.30; H, 5.09; N, 3.50. UV–vis (toluene) λ_{\max}/nm ($\epsilon/\text{M}^{-1}\text{cm}^{-1}$): 341 (5.52 × 10³).

Synthesis of (Cl₃C-Amido-imino)TaCl₄ (5b**).** Carbon tetrachloride (47.5 μ L, 0.49 mmol) was added to a solution of complex **2b** (325 mg, 0.49 mmol) in toluene (5 mL) at room temperature. This reaction mixture was stirred for 4 h at 60 °C, and then all volatiles were removed under reduced pressure to give yellow solid. The solid was washed with hexane (3 × 10 mL) and dried to give **5b** as a yellow powder in 83% yield (332 mg, 0.41 mmol), mp 146–147 °C (dec). ¹H NMR (400 MHz, C₆D₆, 308 K) δ 0.99 (d, *J* = 6.8 Hz, 3H, CH(CH₃)₂), 1.01 (d, *J* = 6.8 Hz, 3H, CH(CH₃)₂), 1.20 (d, *J* = 6.8 Hz, 3H, CH(CH₃)₂), 1.37 (d, *J* = 6.8 Hz, 6H, CH(CH₃)₂), 1.44 (d, *J* = 6.8 Hz, 3H, CH(CH₃)₂), 1.47 (d, *J* = 6.8 Hz, 3H, CH(CH₃)₂), 1.67 (d, *J* = 6.8 Hz, 3H, CH(CH₃)₂), 3.47 (sept, *J* = 6.8 Hz, 1H, CH(CH₃)₂), 3.60 (sept, *J* = 6.8 Hz, 1H, CH(CH₃)₂), 3.76 (sept, *J* = 6.8 Hz, 1H, CH(CH₃)₂), 3.94 (sept, *J* = 6.8 Hz, 1H, CH(CH₃)₂), 7.04 (s, 1H, CCl₃CH), 7.0–7.1 (m, 6H, aromatic protons), 8.98 (s, 1H, N=CH). ¹³C NMR (100 MHz, C₆D₆, 308 K) δ 23.3 (CH(CH₃)₂), 24.2

(CH(CH₃)₂), 25.4 (CH(CH₃)₂), 25.6 (CH(CH₃)₂), 25.8 (CH(CH₃)₂), 25.9 (CH(CH₃)₂), 26.1 (CH(CH₃)₂), 27.5 (CH(CH₃)₂), 28.7 (CH(CH₃)₂), 28.9 (CH(CH₃)₂), 29.4 (CH(CH₃)₂), 30.2 (CH(CH₃)₂), 89.6 (NCH(CCl₃)CH), 101.5 (CCl₃), 124.7 (Ar), 124.9 (Ar), 126.3 (Ar), 128.1 (Ar), 129.5 (Ar), 131.1 (Ar), 141.1 (Ar), 142.3 (Ar), 142.4 (Ar), 145.7 (Ar), 147.9 (Ar), 151.0 (Ar), 180.8 (C=N). Anal. Calcd for C₂₇H₃₆C₁₇N₂Ta (C₆H₅CH₃)_{0.25}: C, 41.07; H, 4.56; N, 3.33. Found: C, 41.12; H, 4.68; N, 3.39.

Complex (Cl₂HC-amido-imino)TaCl₄ (**6b**) was prepared in a similar manner as **5b**. A yellow powder was obtained in 62% yield, mp 132–133 °C (dec). ¹H NMR (400 MHz, C₆D₆, 308 K) δ 0.92 (d, *J* = 6.8 Hz, 3H, CH(CH₃)₂), 1.05 (d, *J* = 6.8 Hz, 3H, CH(CH₃)₂), 1.10 (d, *J* = 6.8 Hz, 3H, CH(CH₃)₂), 1.18 (d, *J* = 6.8 Hz, 3H, CH(CH₃)₂), 1.37 (d, *J* = 6.8 Hz, 3H, CH(CH₃)₂), 1.44 (d, *J* = 6.8 Hz, 3H, CH(CH₃)₂), 1.48 (d, *J* = 6.8 Hz, 3H, CH(CH₃)₂), 1.55 (d, *J* = 6.8 Hz, 3H, CH(CH₃)₂), 3.41 (sept, *J* = 6.8 Hz, 1H, CH(CH₃)₂), 3.72 (sept, *J* = 6.8 Hz, 1H, CH(CH₃)₂), 3.77 (sept, *J* = 6.8 Hz, 1H, CH(CH₃)₂), 4.34 (sept, *J* = 6.8 Hz, 1H, CH(CH₃)₂), 5.52 (d, *J* = 1.8 Hz, 1H, Cl₂CH–), 6.76 (br, 1H, Cl₂CHCH), 7.0–7.15 (m, 6H, aromatic protons), 8.72 (br, 1H, N=CH). ¹³C NMR (100 MHz, C₆D₆, 308 K) δ 23.4 (CH(CH₃)₂), 24.2 (CH(CH₃)₂), 25.2 (CH(CH₃)₂), 25.6 (CH(CH₃)₂), 25.9 (CH(CH₃)₂), 25.9 (CH(CH₃)₂), 26.4 (CH(CH₃)₂), 26.9 (CH(CH₃)₂), 28.5 (CH(CH₃)₂), 28.8 (CH(CH₃)₂), 29.1 (CH(CH₃)₂), 29.3 (CH(CH₃)₂), 71.6 (Cl₂CHCH), 86.4 (Cl₂CH–), 124.6 (Ar), 125.0 (Ar), 126.6 (Ar), 127.3 (Ar), 129.4 (Ar), 130.4 (Ar), 141.2 (Ar), 142.3 (Ar), 145.3 (Ar), 145.7 (Ar), 148.1₁ (Ar), 148.1₂ (Ar), 180.0 (C=N). Anal. Calcd for C₂₇H₃₇Cl₆N₂Ta: C, 41.40; H, 4.76; N, 3.58. Found: C, 41.58; H, 5.21; N, 3.48.

Polymerization of Styrene by Complex 2a. Styrene (0.51 mL, 4.9 mmol) and carbon tetrachloride (4.9 μL, 0.049 mmol) were added to a solution of complex **2a** (34 mg, 0.049 mmol) in toluene (5 mL) at room temperature. The reaction mixture was stirred for 18 h at 60 °C. The mixture was added to excess of MeOH, yielding a white precipitate of poly(styrene) (0.12 g, 26% yield), which was filtered and dried (*M_n* = 1.9 × 10³, *M_w*/*M_n* = 1.3).

Synthesis of (Cl₃CCH₂CH(Ph)-Amido-imino)TaCl₄ (7b**).** Styrene (0.33 mL, 2.9 mmol, 5 equiv) and carbon tetrachloride (0.054 mL, 0.57 mmol) were added to a solution of complex **2b** (0.38 g, 0.57 mmol) in toluene (8 mL) at room temperature. The reaction mixture was stirred for 20 h at 60 °C, and then volatiles were removed under reduced pressure to give yellow solid. The solid was washed with hexane (3 × 10 mL), and the solvent was evaporated to give **7b** as a yellow powder in 54% yield (0.28 g, 0.31 mmol), mp 157–159 °C (dec). ¹H NMR (400 MHz, C₆D₆, 308 K) δ 0.79 (d, *J* = 6.8 Hz, 3H, CH(CH₃)₂), 1.23 (d, *J* = 6.8 Hz, 3H, CH(CH₃)₂), 1.30 (d, *J* = 6.8 Hz, 6H, CH(CH₃)₂), 1.42 (d, *J* = 6.8 Hz, 3H, CH(CH₃)₂), 1.49 (d, *J* = 6.8 Hz, 3H, CH(CH₃)₂), 1.51 (d, *J* = 6.8 Hz, 3H, CH(CH₃)₂), 1.58 (d, *J* = 6.8 Hz, 3H, CH(CH₃)₂), 3.12 (d, *J* = 14.8 Hz, 1H, PhCHCH₂CCl₃), 3.34 (sept, *J* = 6.8 Hz, 1H, CH(CH₃)₂), 3.42 (dd, *J* = 14.8 Hz, *J* = 10.3 Hz, 1H, PhCHCH₂CCl₃), 3.47 (m, *J* = 6.8 Hz, 2H, CH(CH₃)₂), 3.79 (m, *J* = 6.8 Hz, 1H, CH(CH₃)₂), 4.63 (d, *J* = 10.3 Hz, 1H, PhCH), 5.37 (d, *J* = 22.7 Hz, 1H, NCH₂), 5.39 (d, *J* = 22.7 Hz, 1H, NCH₂), 6.88–7.16 (m, 11H, aromatic protons). ¹³C NMR (100 MHz, C₆D₆, 308 K) δ 22.0 (CH(CH₃)₂), 23.6 (CH(CH₃)₂), 24.6 (CH(CH₃)₂), 25.1 (CH(CH₃)₂), 27.3 (CH(CH₃)₂), 27.7 (CH(CH₃)₂), 28.0 (CH(CH₃)₂), 28.6 (CH(CH₃)₂), 28.7 (CH(CH₃)₂), 29.2 (CH(CH₃)₂), 29.2 (CH(CH₃)₂), 29.7 (CH(CH₃)₂), 45.8 (PhCHCH₂CCl₃), 51.2 (PhCHCH₂CCl₃), 74.4 (ArNCH₂), 96.5 (CCl₃), 125.4 (Ar), 125.7 (Ar), 126.3 (Ar), 126.3 (Ar), 128.8 (Ar), 129.1 (Ar), 129.2 (Ar), 129.6 (Ar), 130.0 (Ar), 134.5 (Ar), 141.0 (Ar), 141.6 (Ar), 143.3 (Ar), 144.4 (Ar), 146.9 (Ar), 148.9 (Ar), 194 (C=N). Anal. Calcd for C₃₅H₄₄Cl₇N₂Ta: C, 45.60; H, 4.81; N, 3.04; Found: C, 45.37; H, 5.05; N, 3.33.

Synthesis of (α-Diimine)TaCl₄ (8b**).** A solution of **1b** (298 mg, 0.79 mmol) in toluene (10 mL) was added to a suspension of (TaCl₄)_n (256 mg, 0.79 mmol) in toluene (10 mL) at room temperature. The

color of the solution changed to deep blue. The reaction mixture was stirred for 14 h, and then volatiles were removed under reduced pressure to give a blue solid. The solid was washed with hexane (3 × 10 mL) and then dried to give **8b** as a blue powder in 77% yield (424 mg, 0.61 mmol), mp 184–186 °C (dec). EPR (toluene): *g* = 2.0031 (*A*_{iso} = 7.0 G), *g* = 1.9332 (*A*_{iso} = 58 G). Anal. Calcd for C₂₆H₃₆Cl₄N₂Ta; C, 44.65; H, 5.19; N, 4.01. Found: C, 44.86; H, 5.21; N, 3.98. λ_{max}/nm (ε/M⁻¹ cm⁻¹): 403 (1.33 × 10³), 593 (2.09 × 10³).

(α-Diimine)TaCl₄ (**8a**) was prepared in a similar manner as **8b**. A deep blue powder was obtained in 35% yield, mp 191–192 °C (dec). EPR (toluene): *g* = 1.9313 (*A*_{iso} = 65 G). Anal. Calcd for C₂₈H₄₀Cl₄N₂Ta; C, 46.23; H, 5.54; N, 3.85. Found: C, 45.98; H, 5.42; N, 3.77. λ_{max}/nm (ε/M⁻¹ cm⁻¹): 624 (1.01 × 10³).

(α-Diimine)TaCl₄ (**8c**) was prepared in a similar manner as **8b**. A deep green powder was obtained in 89% yield, mp 213–215 °C (dec). EPR (toluene): *g* = 2.0026 (*A*_{iso} = 6.1 G), *g* = 1.9152 (*A*_{iso} = 60 G). Anal. Calcd for C₃₆H₄₀Cl₄N₂Ta(C₆H₅CH₃); C, 56.41; H, 5.28; N, 3.06. Found: C, 56.53; H, 5.09; N, 3.42. λ_{max}/nm (ε/M⁻¹ cm⁻¹): 336 (1.65 × 10⁴), 686 (3.35 × 10³).

Reduction of Complex 8b Leading to [Cp₂Co][(α-Diimine)TaCl₄] (9b**).** A solution of Cp₂Co (37.8 mg, 0.20 mmol) in toluene (5 mL) was added to solution of complex **8b** (139 mg, 0.20 mmol) in toluene (5 mL) at room temperature. The color of the mixture turned to green. After 3 h of stirring, the volatiles were removed under reduced pressure to give a green solid that was washed with hexane (3 × 10 mL). The remaining solid was dried to give **9b** as a green powder in 92% yield (163 mg, 0.18 mmol), mp 218–220 °C (dec). ¹H NMR (400 MHz, CDCl₃, 308 K) δ 1.16 (d, *J* = 6.5 Hz, 12H, CH(CH₃)₂), 1.39 (d, *J* = 6.5 Hz, 12H, CH(CH₃)₂), 4.29 (sept, *J* = 6.5 Hz, 4H, CH(CH₃)₂), 4.84 (br s, 2H, CH=CH), 5.51 (br s, 10H, Cp₂Co), 7.09 (br d, 2H, *p*-Ar), 7.19 (br t, 4H, *o*-Ar). ¹³C NMR (400 MHz, CDCl₃, 308 K) δ 23.8 (CH(CH₃)₂), 26.7 (CH(CH₃)₂), 27.9 (CH(CH₃)₂), 85.1 (Cp₂Co), 122.6 (HC=CH), 123.7 (*m*-Ar), 126.6 (*p*-Ar), 146.8 (Ar), 150.2 (Ar). Anal. Calcd for C₃₆H₄₆Cl₄CoN₂Ta; C, 48.67; H, 5.22; N, 3.15. Found: C, 49.18; H, 5.58; N, 2.99. λ_{max}/nm (ε/M⁻¹ cm⁻¹): 395 (5.51 × 10³).

Oxidation of Complex 8b Leading to [(α-Diimine)TaCl₄]-[WCl₆] (10b**).** A solution of WCl₆ (86.6 mg, 0.22 mmol) in toluene (5 mL) was added to solution of complex **8b** (154 mg, 0.22 mmol) in toluene (5 mL) at room temperature. The color of the mixture turned to red. After stirring for 3 h, the volatiles were removed under reduced pressure to give reddish-brown solid. The solid was washed with hexane (3 × 10 mL), and dried vacuum to give **10b** as reddish-brown powder in 45% yield (108 mg, 0.10 mmol), mp 134–136 °C (dec). ¹H NMR (400 MHz, CDCl₃, 308 K) δ 1.15 (d, *J* = 6.5 Hz, 12H, CH(CH₃)₂), 1.23 (d, *J* = 6.5 Hz, 12H, CH(CH₃)₂), 3.02 (sept, *J* = 6.5 Hz, 4H, CH(CH₃)₂), 7.26 (m, 6H, aromatic protons), 9.53 (br s, 2H, N=CH). ¹³C NMR (400 MHz, CDCl₃, 308 K) δ 23.6 (CH(CH₃)₂), 28.0 (CH(CH₃)₂), 30.5 (CH(CH₃)₂), 125.9 (Ar), 131.6 (*p*-Ar), 142.4 (Ar), 148.7 (Ar), 181.7 (N=C). Anal. Calcd for C₂₆H₃₆Cl₁₀N₂TaW(C₆H₅CH₃)_{0.5}; C, 31.03; H, 3.53; N, 2.45. Found: C, 31.42; H, 3.78; N, 2.51. λ_{max}/nm (ε/M⁻¹ cm⁻¹): 344 (1.69 × 10⁴).

Oxidation of Complex 9b Leading to (α-Diimine)TaCl₄ (8b**).** A solution of WCl₆ (30.2 mg, 0.08 mmol) in toluene (5 mL) was added to a solution of complex **9b** (68.0 mg, 0.08 mmol) in toluene (5 mL) at –78 °C. The reaction mixture was allowed to slowly warm to ambient temperature and was stirred for 3 h. The precipitate was filtered, and volatiles were removed under reduced pressure to give **8b** as a deep blue powder in 60% yield (33.6 mg, 0.05 mmol). The complex **8b** was characterized by EPR spectroscopy (see Figure S18a in Supporting Information).

Reduction of Complex 10b Leading to (α-Diimine)TaCl₄ (8b**).** A solution of Cp₂Co (19.4 mg, 0.10 mmol) in toluene (5 mL) was added to a solution of complex **10b** (112 mg, 0.10 mmol) in toluene (5 mL) at –78 °C. The reaction mixture was allowed to slowly warm to ambient temperature and was stirred for 3 h. The precipitate was filtered, and volatiles were removed under reduced pressure to give **8b** as a deep blue powder in 54% yield (36.3 mg, 0.05 mmol). The complex **8b** was

characterized by EPR spectroscopy (see Figure S18b in Supporting Information).

Decomposition of NaBPh₄ by (α -Diimine)TaCl₄ (8b). NaBPh₄ (45.0 mg, 0.13 mmol) was added to a solution of **8b** (92.7 mg, 0.13 mmol) in CH₂Cl₂ (5 mL) at room temperature. The reaction mixture was stirred for 24 h, over which time the color of the mixture gradually changed to yellow. Naphthalene (18.0 mg, 0.14 mmol) was then added to the reaction mixture as an internal standard for GC measurement. The solution was quenched with water and the organic layer was analyzed by GC and GC–MS. Biphenyl was produced in 52% yield (as determined by GC analysis). Formation of **8b** was confirmed by the ¹H NMR spectrum (see Figure S2 and S3 in Supporting Information). A similar reaction was observed for the mixture of **8a** and NaBPh₄.

Reaction of Complex **8a with AIBN Leading to **4a**.** Azobisisobutyronitrile (26 mg, 0.16 mmol) was added to a solution of complex **8a** (230 mg, 0.31 mmol) in toluene (5 mL) at room temperature. The reaction mixture was stirred for 20 h at 60 °C, and then all volatiles were removed under reduced pressure to give a red powder. The powder was washed with hexane (3 × 10 mL), and the remaining solid was dried to give yellow powder of **4a** in 72% yield (160 mg, 0.22 mmol). The ¹H NMR spectrum was consistent with that of **4a**.

X-ray Crystallographic Analysis. All crystals were handled similarly. The crystals were mounted on the CryoLoop (Hampton Research Corp.) with a layer of light mineral oil and placed in a nitrogen stream at 113(1) K. Measurements were made on Rigaku R-Axis RAPID imaging plate area detector or Rigaku AFC7R/Mercury CCD detector with graphite-monochromated Mo K α (0.71075 Å) radiation. Crystal data and structure refinement parameters were listed below (Table S1 in Supporting Information).

The structures of complexes **2b**, **3c**, **7b**, **8b**, **8c**, and **9b** were solved by direct methods (SHELXS-97).¹⁴ The structure of complex **8a** was solved by direct methods (SIR92).¹⁵ The structures were refined on F^2 by full-matrix least-squares method, using SHELXL-97.¹⁴ Non-hydrogen atoms were anisotropically refined. Hydrogen atoms were included in the refinement on calculated positions riding on their carrier atoms. The function minimized was $[\sum w(F_o^2 - F_c^2)^2]$ ($w = 1/[\sigma^2(F_o^2) + (aP)^2 + bP]$), where $P = (\text{Max}(F_o^2, 0) + 2F_c^2)/3$ with $\sigma^2(F_o^2)$ from counting statistics. The function R1 and wR2 were $(\sum ||F_o| - |F_c||)/\sum |F_o|$ and $[\sum w(F_o^2 - F_c^2)^2/\sum (wF_o^4)]^{1/2}$, respectively. For the complex **3c**, large solvent accessible voids in the lattice were involved in the crystal packing, but we could not find suitable solvent molecules due to the disordered density. The molecular structure of **3c** was shown in the Supporting Information. The ORTEP-3 program was used to draw the molecule.¹⁶

RESULTS AND DISCUSSION

Preparation of Tantalum Complexes with Dianionic α -Diimine Ligands. Reduction of TaCl₅ by MBTCD in the presence of α -diimine ligands **1a** and **1b** resulted in the formation of tantalum complexes **2a** and **2b** (Scheme 1). In the NMR spectra of **2a** and **2b**, resonances assignable to alkene carbons were observed at δ_C 110.0 for **2a** and 104.8 for **2b**, and the signal for an imine proton for **1b** was shifted to higher field (δ_H 5.67), indicating the reduction of neutral α -diimine ligands **1a** and **1b** to dianionic ene-diamide ligands. An X-ray diffraction study of **2b** reveals a dianionic ene-diamido coordination mode to the tantalum atom (Figure 1).¹⁷ The C1–N1 bond length (1.376(9) Å), the C1–C1* bond length (1.406(13) Å), and the fold angle between the N1–C1–C1*–N1 and N1–Ta–N1* planes (123.0°) are typical for dianionic ligation to early transition metal centers.^{17,18} Thus, during the complexation reaction, the α -diimine ligands were reduced by in situ generated “TaCl₃”.

Scheme 1. Preparation of Tantalum Complexes with Dianionic α -Diimine Ligands Using MBTCD as a Reductant

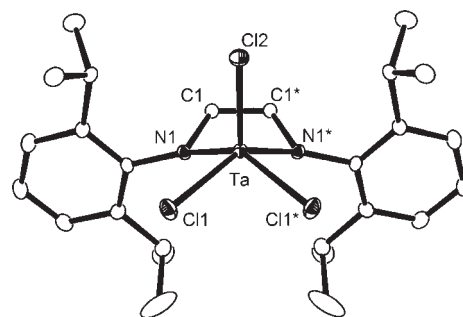
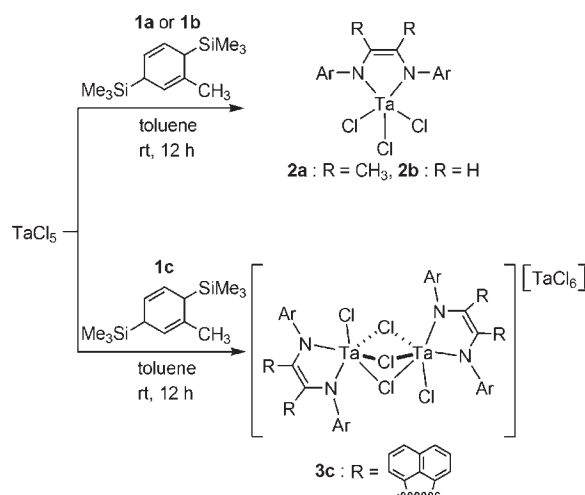
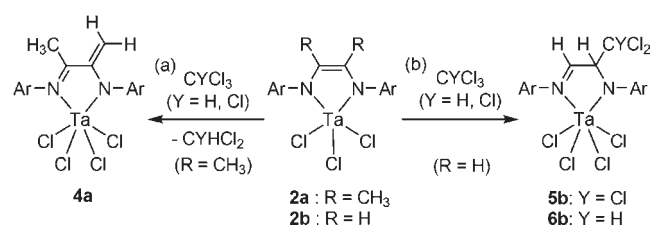


Figure 1. Molecular structure of **2b** with 30% thermal ellipsoids. All hydrogen atoms are omitted for clarity. Selected bond distances (Å) and angles (deg): Ta–N1, 1.968(6); Ta–Cl1, 2.3778(18); Ta–Cl2, 2.281(3); Ta–Cl1, 2.428(7); N1–C1, 1.376(9); C1–C1*, 1.406(13). Dihedral angle between N1–C1–C1*–N1* planes = 123.0°.

In contrast, the reaction of in situ generated “TaCl₃” with an acenaphthene-based α -diimine ligand **1c** gave a less soluble tantalum complex **3c**. The preliminary X-ray diffraction study of **3c** revealed the formation of the chloride-bridged dimeric complex, $[(\alpha\text{-diimine})\text{TaCl}_2(\mu\text{-Cl})_3][\text{TaCl}_6]$.¹⁹ The ¹³C NMR spectrum of **3c** displayed a resonance for the N-bound acenaphthylene carbon at δ 109.7, indicating the two electron reduction of **1c**.

Reductive Cleavage of C–Cl Bonds by (α -Diimine)TaCl₃. The complexes **2a** and **2b** showed unique reactivity toward alkyl halides: reactions of CCl₄ and CHCl₃ with **2a** afforded the same TaCl₄ complex **4a** in good yields (Scheme 2a). By monitoring the reaction of **2a** with polyhaloalkanes using ¹H NMR spectroscopy, we found generation of dehalogenated products, CHCl₃ and CH₂Cl₂, respectively, in the reaction mixtures. In the ¹H NMR spectrum of **4a**, two broad doublet resonances were observed at δ 4.62 and 5.33 due to the vinylidene moiety of the ligand backbone, indicating an in situ generated radical from polyhaloalkanes abstracted the hydrogen atom of the ligand backbone. Similarly, complex **2b** also activated a carbon–chloride bond of CCl₄ or CHCl₃ to form a TaCl₄ fragment; however,

Scheme 2. Reductive Cleavage of C–Cl Bond of Polyhaloalkanes



the organic residual fragments attached to the ligand backbone, to give the corresponding amido-imino complexes **5b** and **6b** (Scheme 2b).²⁰ The ¹³C NMR spectra of **5b** and **6b** displayed singlet resonances corresponding to trichloromethyl and dichloromethyl groups at δ 101.5 for **5b** and 86.4 for **6b**. In both reactions in Scheme 2, the carbon–chlorine bond was activated by a high-valent d⁰ metal complex. We assume that the initial step was one electron transfer from the dianionic ene-diamide ligand in **2a** or **2b** to the polyhaloalkane to generate tantalum tetrachloride complexes of π -radical monoanionic α -diimine ligands and organic radicals (vide infra). If the generated organic radicals attacked the metal center of **2a** or **2b** (which were still present in the reaction mixture), new organometallic species were produced via formation of new tantalum–carbon bonds. Reversible metal–carbon bond formation and homolytic cleavage processes are known to feature in organometallic mediated radical polymerization reactions.²¹ However, attacking the ligand backbone is preferable to form complexes **4a**, **5b**, and **6b**.

Another reaction pathway between the carbon radical and metal halides is a halogen abstraction reaction from the metal center to generate alkyl halides. Such C–X bond formation is an important step for atom transfer radical addition and polymerization reactions.²² We thus examined a radical polymerization reaction of styrene by the in situ generated radical from the reaction of **2a** or **2b** with polyhaloalkanes. Treatment of catalytic amounts of **2a** and CCl₄ in the presence of excess styrene resulted in the formation of poly(styrene) (26% yield, $M_n = 1.9 \times 10^3$, $M_w/M_n = 1.3$) and unidentified tantalum species, indicating the generated trichloromethyl radical initiated radical polymerization of styrene (Scheme 3a). When PhCH₂Br was used as the initiator for the styrene polymerization reaction, poly(styrene) was obtained in 53% yield ($M_n = 1.6 \times 10^3$, $M_w/M_n = 1.4$). The slightly increased yield of the polymer is probably due to the low concentration of the carbon radical from **2a**/PhCH₂Br.²³ In the ¹H NMR spectra of the poly(styrene), resonances assignable to the terminal proton adjacent to the halogen atom were not observed,²⁴ suggesting the free-radical polymerization character and the difficulty of the abstraction of halides bound to the high-valent early transition metal center by carbon radicals.²⁵ In contrast, the reaction of **2b**, CCl₄, and styrene (5 equiv) gave a new tantalum complex **7b**, which was characterized using ¹H and ¹³C NMR spectra, aided by 2D NMR measurements (Scheme 3b). The ¹H NMR spectrum of **7b** displayed two doublet resonances assignable to the amidomethylene group at δ 5.37 and 6.39 ($J = 22.7$ Hz). The resonance for the imine carbon was observed at δ 194.0, whereas the signal due to the imine proton was not detected in the ¹H NMR spectrum, suggesting intramolecular hydrogen transfer in the ligand backbone.²⁶ It was noteworthy that one ABX type signal appeared at δ 3.12, 3.42, and 4.63 ($J = 9.8$ and 14.8 Hz) assignable to a 1-phenyl-3,3,3-trichloropropyl group, which was generated by the addition of trichloromethyl radical to styrene.

Scheme 3. Radical Addition Reaction of Trichloromethyl Radical to Styrene

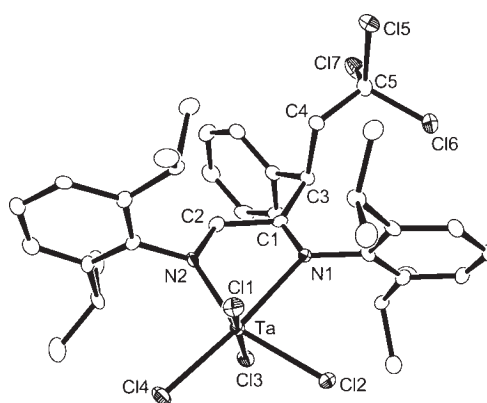
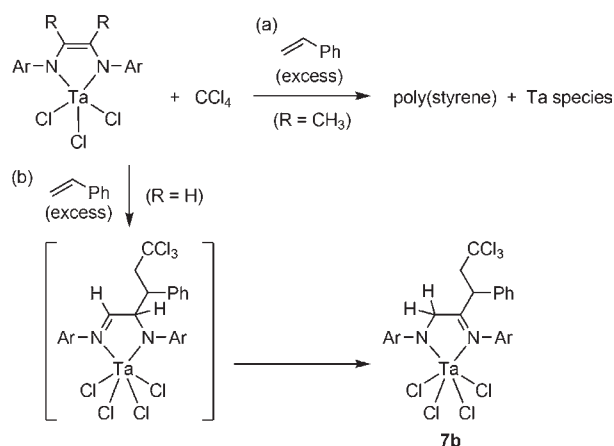
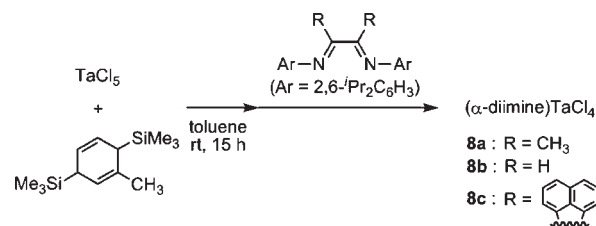


Figure 2. Molecular structure of **7b** with 30% thermal ellipsoids. All hydrogen atoms are omitted for clarity. Selected bond distances (Å) and angles (deg): Ta–N1, 2.395(6); Ta–N2, 1.971(6); Ta–Cl1, 2.323(3); Ta–Cl2, 2.360(2); Ta–Cl3, 2.392(3); Ta–Cl4, 2.304(2); N1–C1, 1.292(10); N2–C2, 1.451(10); C1–C2, 1.504(10); C1–C3, 1.535(11); C3–C4, 1.546(11); N1–Ta–N2, 72.2(2); N1–Ta–Cl2, 80.91(14); N1–Ta–Cl4, 169.06(18); N2–Ta–Cl2, 153.06(16); N2–Ta–Cl4, 100.27(16).

Scheme 4. Synthesis of (α -Diimine)TaCl₄ Complexes

Formation of poly(styrene) or incorporation of several styrene molecules into the ligand backbone was not observed for the reaction of **2b** and CCl₄ in the presence of excess styrene, indicating that the radical coupling reaction of benzyl radical with the π -radical ligand was faster than the radical addition to another styrene monomer.²⁷ We monitored the reaction of **2b** with CCl₄ in the presence of styrene by ¹H NMR spectroscopy. When excess styrene (100 equiv) was added

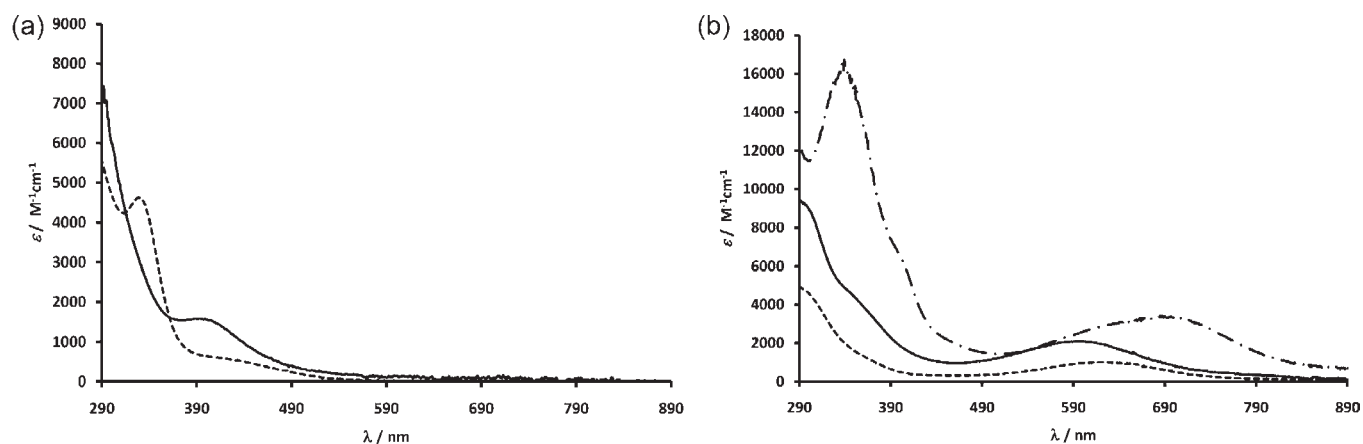


Figure 3. UV-vis spectra of tantalum complexes in toluene at 25 °C. (a) 2a (----) and 2b (—). (b) 8a (.....), 8b (—), and 8c (— · —).

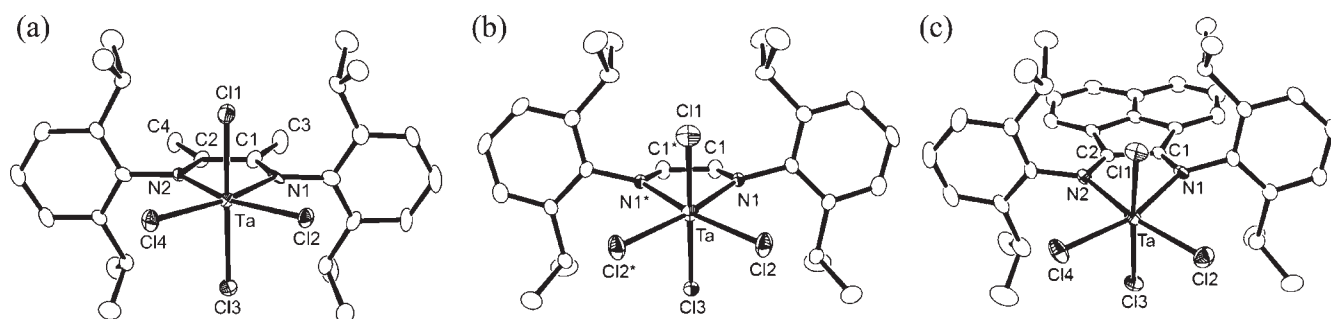


Figure 4. Molecular structures of (α -diimine) TaCl_4 ((a) 8a, (b) 8b, and (c) 8c) with 30% thermal ellipsoids. All hydrogen atoms are omitted for clarity.

Table 1. Bond Distances (Å) and Angles (deg) of 8a–8c

	8a	8b	8c
Ta–N1	2.195(8)	2.154(3)	2.164(3)
Ta–N2	2.148(7)		2.179(3)
Ta–Cl1	2.326(3)	2.3199(15)	2.3521(10)
Ta–Cl2	2.364(2)	2.3176(11)	2.3106(10)
Ta–Cl3	2.379(4)		2.3153(10)
Ta–Cl4	2.276(2)		2.3554(11)
N1–C1	1.326(10)	1.333(4)	1.332(4)
N2–C2	1.342(10)		1.333(4)
C1–C2	1.434(11)	1.425(7)	1.442(4)
N1–Ta–N2	71.8(3)	74.44(15) ^a	74.79(10)
N1–Ta–Cl1	93.9(2)	94.44(8)	89.83(8)
N1–Ta–Cl2	87.4(2)	90.56(8)	91.51(8)

^a N1–Ta–N1*

and the reaction mixture was heated at 60 °C, complex **7b** was formed as the main product together with the formation of **5b** (**5b/7b** = 13/87). In the case where an equimolar amount of styrene was added to the reaction mixture, complex **5b** was the main product (**5b/7b** = 63/37), suggesting that the product ratio (**5b/7b**) was dependent on the amount of styrene and the intramolecular radical coupling to form **5b** was favorable compared to intermolecular reaction.

The molecular structure of **7b** was confirmed by X-ray diffraction (Figure 2). The tantalum center is pseudo-octahedral with four chloride and one amido-imino ligands. The Ta–N1 distance (2.395(6) Å) is in the range typically observed for

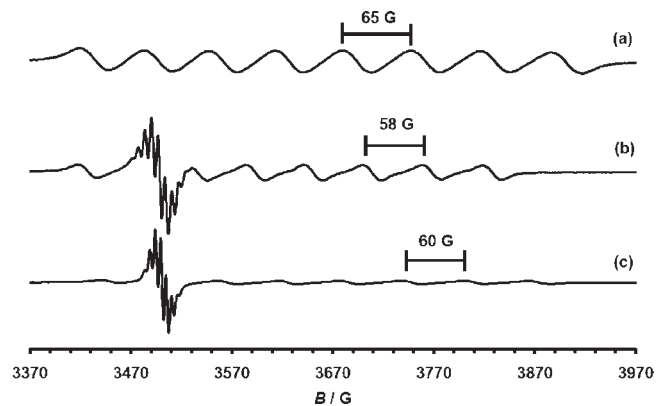


Figure 5. EPR spectra in toluene at room temperature for (a) 8a, (b) 8b, and (c) 8c.

tantalum–nitrogen dative bonds, while N2 bound to the metal center as an amido nitrogen atom as evident from the short Ta–N2 bond length (1.971(6) Å).^{17,28} The C2–N2 interaction is longer than that of C1–N1, indicating intramolecular hydrogen transfer to form a saturated CH₂ moiety in the ligand backbone.²⁶ The trichloromethyl group is bound to the β -position of the imine group due to the addition of trichloromethyl radical to the α -position of styrene.

Preparation and Structure of (α -Diimine) TaCl_4 . In the reactions described in Schemes 2 and 3, tetrachlorotantalum complexes were regarded as key intermediates. We thus examined the preparation of (α -diimine) TaCl_4 complexes. Reaction of TaCl_5

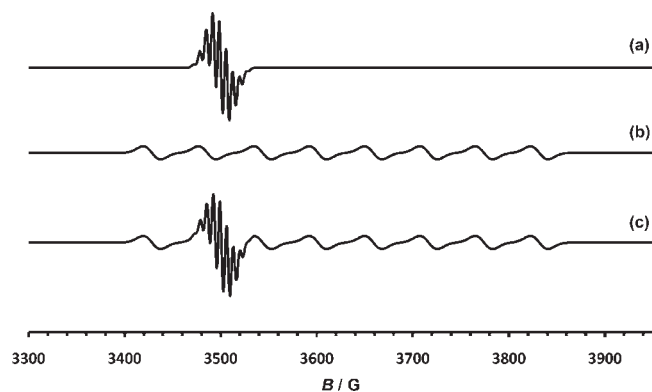
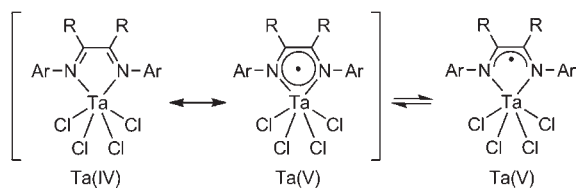


Figure 6. (a) Simulated spectrum of **8b** for ligand-centered radical species ($g = 2.0031$, $a_N = 6.80$ G, $a_H = 6.31$ G). (b) Simulated spectrum of **8b** for tantalum-centered radical species ($g = 1.9332$, $a_{Ta} = 57.6$ G). (c) Addition spectrum of simulated spectra for ligand- and tantalum-centered radical species.

Chart 2. Coordination Mode of α -Diimine Ligands for (α -Diimine) $TaCl_4$



with a 0.5 equiv of MBTCD resulted in the formation of $(TaCl_4)_n$ species, which were treated with the α -diimine ligands **1a–1c** to yield deep blue to green powders **8a–8c** (Scheme 4). Figure 3 shows the UV–vis spectra of **2a** and **2b** and **8a–8c** in toluene. The absorption maxima in the visible region at 624, 593, and 686 nm ($\epsilon > 10^3$ M $^{-1}$ cm $^{-1}$) for **8a–8c** are characteristic of the presence of a ligand π radical anion;^{5h,8b} the corresponding absorption band was not observed for the UV–vis spectra of **2a** and **2b**.

The 1H NMR spectra of **8a–8c** displayed only broad resonances; the molecular structures were therefore elucidated using X-ray diffraction. ORTEP drawings of the structures are shown in Figure 4, and the selected geometries are summarized in Table 1. In contrast to the structure of **2b**, the five-membered metallacycles formed by the α -diimine ligands and tantalum atom are in the same plane. The Ta–N distances range from 2.148(7) to 2.195(8) Å and are slightly longer than other tantalum–nitrogen σ -bonds.²⁸ The C–N and C–C bond lengths of the α -diimine ligands deviate from those of the free ligands²⁹ and dianionic enediamido ligands. The elongated C–N (ca. 1.33 Å) and shortened C–C (ca. 1.43 Å) bonds suggest the partial reduction of the α -diimine ligand to form a ligand-centered π -radical.^{5d,h,i,k,l,o,8b,30}

EPR Spectra of (α -Diimine) $TaCl_4$. The EPR spectra of **8a–8c** clearly reflected the coordination mode of the α -diimine ligands to the tantalum atom. The EPR spectrum of **8a** displayed an eight-line pattern due to the isotropic tantalum nuclear spin ($g = 1.9313$, $A_{iso} = 65$ G) (Figure 5a). The isotropic hyperfine coupling constant is lower than that of the purely localized tantalum-centered radical complexes, $TaCl_4(PET_3)_2$ ($A_{iso} = 211$ G)³¹ and $Ta(\eta-C_6H_6)_2$ ($A_{iso} = 138$ G),³² and is correlated to the electron density of the metal center, as observed for

Scheme 5. Chemical Oxidation and Reduction Reactions of **8b**

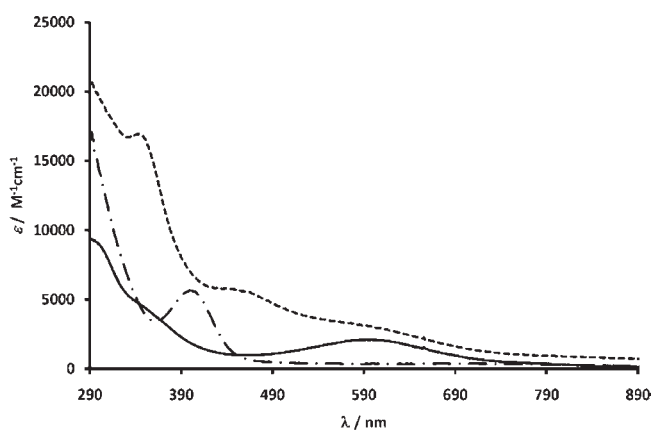
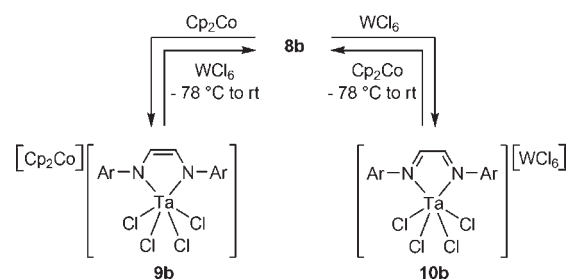


Figure 7. UV–vis spectra of **8b** (—), **9b** (---) and **10b** (····) in CH_2Cl_2 at 25 °C.

$(C_5R_5)Ta(C_7H_7)$ complexes ($A_{iso} = 61–113$ G).³³ Thus, the relatively lower value of the coupling constant for **8a** might be ascribed to the two resonance structures of tantalum(IV)-localized and TaN_2C_2 metallacycle-delocalized unpaired electron of **8a**;^{6h} no superhyperfine coupling due to the nitrogen atoms of the ligand backbone was resolved. In contrast, two resonances were observed for **8b**: an eight-line pattern, $g = 1.9332$, $A_{iso} = 58$ G and a nine-line pattern, $g = 2.0031$, $A_{iso} = 7.0$ G (Figure 5b). The nine-line splitting resonance is simulated by taking into account hyperfine coupling with two virtually identical nitrogen atoms ($a_N = 6.80$ G) and four equivalent hydrogen atoms of the $N=CH$ and p -hydrogen atom of the N -aryl group ($a_H = 6.31$ G) (Figure 6a). The eight-line patterned signal is simulated as a tantalum-centered radical ($a_{Ta} = 57.6$ G) (Figure 6b). Accordingly, the EPR spectrum of **8b** is consistent with sets of two signals: one corresponds to two resonance structures of tantalum(IV)-localized and TaN_2C_2 metallacycle-delocalized radical, and the other is an organic radical purely localized on the α -diimine ligands.^{20,34} The strength of the signal for the π -radical monoanionic ligand was controllable by extending the π -aromatic backbone of α -diimine ligands. Analogous to the EPR spectrum of **8b**, two signals were observed for **8c** (Figure 5c, eight-line pattern, $g = 1.9152$, $A_{iso} = 60$ G; seven-line pattern, $g = 2.0026$, $A_{iso} = 6.1$ G).³⁵ Based on the EPR spectra of **8a–8c**, the coordination modes of the α -diimine ligands of **8a–8c** are shown as neutral or π -radical α -diimine ligands, as shown in Chart 2.³⁶ Therefore, formation of **5b** and **6b** is consistent with coupling of the carbon radical and the ligand-localized π -radical. On the other hand, an unpaired electron in **4a** mainly localized

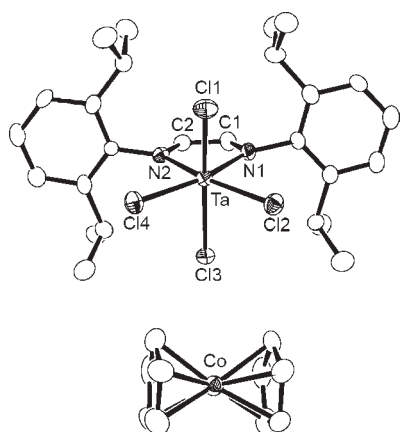


Figure 8. Molecular structure of $[\text{Cp}_2\text{Co}][(\alpha\text{-diimine})\text{TaCl}_4]$ (**9b**) with 30% thermal ellipsoids. All hydrogen atoms are omitted for clarity.

Table 2. Bond Distances (Å) and Angles (deg) of **9b**

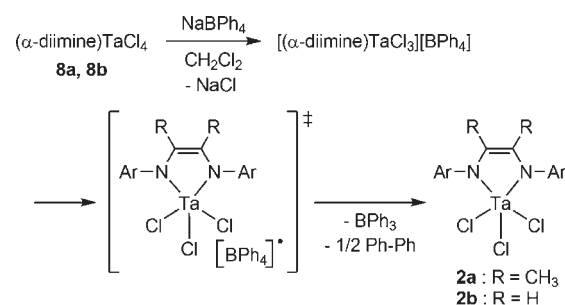
Ta–N1	2.068(7)	Ta–N2	2.075(7)
Ta–Cl1	2.405(2)	Ta–Cl2	2.402(2)
Ta–Cl3	2.4079(19)	Ta–Cl4	2.371(2)
N1–C1	1.391(10)	N2–C2	1.390(10)
C1–C2	1.356(11)		
N1–Ta–N2	75.4(3)		
N1–Ta–Cl1	97.25(19)		
N1–Ta–Cl2	89.30(19)		

on the tantalum atom, and thus the carbon radical abstracted one hydrogen atom from the ligand backbone in Scheme 2a.

Redox Reactivity of (α -Diimine) TaCl_4 . The redox properties of (α -diimine) TaCl_4 complexes were investigated using cyclic voltammetry.³⁵ In all cases, two reversible one-electron redox processes, $[\mathbf{8}]/[\mathbf{8}]^-$ and $[\mathbf{8}]/[\mathbf{8}]^+$, were observed. The one-electron reduction potential was almost the same among complexes **8a–8c**, whereas the difference of the oxidation potential was ca. 0.2 V ($E_{1/2}^{\text{ox}} = -0.01$ V for **8a** and 0.21 V for **8c** vs $[\text{Cp}_2\text{Fe}]^{+/0}$). On the basis of the reversibility of the redox processes, we examined the chemical oxidation and reduction of **8c** using Cp_2Co as a reductant and WCl_6 as an oxidant. Reduction of **8b** with Cp_2Co resulted in the formation of ligand-centered reduced species **9b** as a green powder in 97% yield. The ligand-centered oxidized species **10b** was formed as a red-brown powder in 68% yield by oxidation of **8b** using WCl_6 (Scheme 5). The ligand-centered redox products **9b** and **10b** were characterized by ^1H and ^{13}C NMR spectra. The resonances due to the hydrogen atoms of the ligand backbone were observed at δ 4.84 for **9b** and δ 9.53 for **10b**, clearly indicating the ligand-based redox reaction to produce dianionic enediamido and neutral α -diimine ligands. UV–vis spectra of complexes **8b**, **9b**, and **10b** are shown in Figure 7. In contrast to **8b** having a π -radical monoanionic ligand, an intense absorption band in the visible region was not observed for **9b**.³⁷ The complex **10b** has broad absorbance in the visible region, probably due to the presence of W(V) anion in the reaction mixture. These chemical redox processes are reversible, and oxidation of **9b** by 1 equiv of WCl_6 or reduction of **10b** by 1 equiv of Cp_2Co at low temperature resulted in the regeneration of **8b**.^{35,38}

Single crystals of **9b** were obtained from saturated chloroform solution; the molecular structure was clarified by X-ray diffraction

Scheme 6. Reduction of Complexes **8a** and **8b** by NaBPh_4



Scheme 7. Reaction of **8a** with AIBN-Derived Carbon Radical

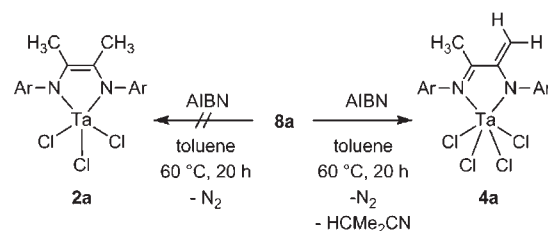


(Figure 8). The bond distances and angles are summarized in Table 2. The tantalum center again is pseudo-octahedral. The Ta–N bonds are shorter than those of **8a–8c**, with values in the range observed for related tantalum–nitrogen σ -bonds.²⁸ Due to the electron-rich character of the tantalum atom of **9b**, the Ta–N bonds are elongated compared with **2b**. In contrast to the structure of **2b**, the TaN_2C_2 metallacycle is almost planar. It is noteworthy that structural features of the α -diimine ligand are typical of early transition metal complexes, with a long–short–long bonding sequence, N1–C1 (1.391(10) Å), C1–C2 (1.356(11) Å), and N2–C2 (1.390(10) Å), reflecting a dianionic σ^2 -enediamido canonical form.¹⁷

Reversibility of the redox processes of α -diimine ligands was also shown by the reaction of **8a** or **8b** with NaBPh_4 . In this reaction, the α -diimine ligands acted as an electron acceptor from the organoborate anion. Reaction of **8a** or **8b** with NaBPh_4 in CH_2Cl_2 resulted in the formation of **2a** or **2b** and biphenyl. During these reactions, the α -diimine ligands in **8a** and **8b** were reduced to form a dianionic ene-diamide ligand (Scheme 6).³⁵ In the presence of oxidants, organoborate anions were decomposed via single electron transfer to form organoborate radical,^{39,40} and thus the electron transfer reaction was assumed to proceed after the formation of ionic species, $[(\alpha\text{-diimine})\text{TaCl}_3][\text{BPh}_4]$.

Next, we examined the reaction of **8a** with AIBN as a source of a carbon radical. In this case the generated carbon radical abstracts a chloride atom bound to the tantalum center, and similar to the reaction in Scheme 6, one-electron reduction of **8a** proceeds to regenerate a dianionic α -diimine ligand. However, the AIBN-derived carbon radical abstracted a hydrogen atom from the ligand backbone of **8a** to give **4a** (Scheme 7).⁴¹ As mentioned in the mechanism for styrene polymerization, abstraction of a halide ligand from early transition metal complexes is difficult compared to H-abstraction or radical recombination reaction.

CONCLUSION

Our results show that (α -diimine)TaCl₃ complexes, involving dianionic α -diimine ligands, induced generation of carbon radicals by reductive cleavage of the C–X bond of polyhaloalkanes. During the reaction, the dianionic ligand is oxidized, releasing one electron to the polyhaloalkane. The radical generated in this process either abstracted a hydrogen atom from the ligand or added to the monoanionic ligand backbone or styrene. Accordingly, these ligand-centered redox processes provide interesting protocols for activating polyhaloalkanes to generate synthetically useful carbon-centered radicals. Recombination of a carbon radical and a halide ligand is difficult due to the strength of the early transition metal–halide bond, but by tuning the electronic property of the supporting ligand to weaken the metal–halogen bond, ligand-based reduction of alkyl halides provides a new strategy for creating early transition metal catalyzed atom transfer radical coupling catalysts.

ASSOCIATED CONTENT

S Supporting Information. Experimental details, selected EPR spectra, cyclic voltammograms, and CIF file of data for complexes **2b**, **3c**, **7b**, **8a**, **8b**, **8c**, and **9b**. This material is available free of charge via the Internet at <http://pubs.acs.org>.

AUTHOR INFORMATION

Corresponding Author

mashima@chem.es.osaka-u.ac.jp

ACKNOWLEDGMENT

T.S. expresses his special thanks for the financial support provided by the JSPS Research Fellowships for Young Scientists. H.T. acknowledged financial support by a Grant-in-Aid for Mitsubishi Chemical Corporation Fund. This work was supported by the Core Research for Evolutional Science and Technology (CREST) program of the Japan Science and Technology Agency (JST), Japan. J.A. thanks the US-NSF for funding (0848931). This paper is dedicated to Professor Christian Bruneau on the occasion of his 60th birthday.

REFERENCES

- (1) (a) Curran, D. P. *Comprehensive Organic Synthesis*; Pergamon: New York, 1992; p 715. (b) Crabtree, R. H. *The Organometallic Chemistry of the Transition Metals*; Wiley Interscience: New York, 2005.
- (2) (a) Kaim, W. *Coord. Chem. Rev.* **1987**, *76*, 187. (b) Jazdzewski, B. A.; Tolman, W. B. *Coord. Chem. Rev.* **2000**, *200–202*, 633. (c) Pierpont, C. G. *Coord. Chem. Rev.* **2001**, *216–217*, 99. (d) Butin, K. P.; Beloglazkina, E. K.; Zyk, N. V. *Russ. Chem. Rev.* **2005**, *74*, 531. (e) Zanello, P.; Corsini, M. *Coord. Chem. Rev.* **2006**, *250*, 2000. (f) Ray, K.; Petrenko, T.; Wieghardt, K.; Neese, F. *Dalton Trans.* **2007**, 1552. (g) Kaim, W.; Schwederski, B. *Coord. Chem. Rev.* **2010**, *254*, 1580.
- (3) (a) Chirik, P. J.; Wieghardt, K. *Science* **2010**, *327*, 794. (b) Bart, S. C.; Lobkovsky, E.; Chirik, P. J. *J. Am. Chem. Soc.* **2004**, *126*, 13794. (c) Bart, S. C.; Hawrelak, E. J.; Lobkovsky, E.; Chirik, P. J. *Organometallics* **2005**, *24*, 5518. (d) Bouwkamp, M. W.; Bowman, A. C.; Lobkovsky, E.; Chirik, P. J. *J. Am. Chem. Soc.* **2006**, *128*, 13340. (e) Bart, S. C.; Chlopek, K.; Bill, E.; Bouwkamp, M. W.; Lobkovsky, E.; Neese, F.; Wieghardt, K.; Chirik, P. J. *J. Am. Chem. Soc.* **2006**, *128*, 13901. (f) Trovitch, R. J.; Lobkovsky, E.; Chirik, P. J. *Inorg. Chem.* **2006**, *45*, 7252. (g) Bart, S. C.; Bowman, A. C.; Lobkovsky, E.; Chirik, P. J. *J. Am. Chem. Soc.* **2007**, *129*, 7212. (h) Trovitch, R. J.; Lobkovsky, E.; Bill, E.; Chirik, P. J. *Organometallics* **2008**, *27*, 1470. (i) Sylvester, K. T.; Chirik, P. J. *J. Am. Chem. Soc.* **2009**, *131*, 8772. (j) Tondreau, A. M.; Milsmann, C.; Patrick, A. D.; Hoyt, H. M.; Lobkovsky, E.; Wieghardt, K.; Chirik, P. J. *J. Am. Chem. Soc.* **2010**, *132*, 15046.
- (4) (a) Dzik, W. L.; van der Vlugt, J. I.; Reek, J. N. H.; de Bruin, B. *Angew. Chem., Int. Ed.* **2011**, *50*, 3356. (b) Smith, A. L.; Hardcastle, K. I.; Soper, J. D. *J. Am. Chem. Soc.* **2010**, *132*, 14358.
- (5) (a) Shaffer, D. W.; Ryken, S. A.; Zarkesh, R. A.; Heyduk, A. F. *Inorg. Chem.* **2011**, *50*, 13. (b) Lu, C. C.; Weyhermüller, T.; Bill, E.; Wieghardt, K. *Inorg. Chem.* **2009**, *48*, 6055. (c) van Gestel, M.; Lu, C. C.; Wieghardt, K.; Lubitz, W. *Inorg. Chem.* **2009**, *48*, 2626. (d) Khusniyarov, M. M.; Weyhermüller, T.; Bill, E.; Wieghardt, K. *J. Am. Chem. Soc.* **2009**, *131*, 1208. (e) Spikes, G. H.; Milsmann, C.; Bill, E.; Weyhermüller, T.; Wieghardt, K. *Inorg. Chem.* **2008**, *47*, 11745. (f) Roy, N.; Sproules, S.; Bill, E.; Weyhermüller, T.; Wieghardt, K. *Inorg. Chem.* **2008**, *47*, 10911. (g) Spikes, G. H.; Sproules, S.; Bill, E.; Weyhermüller, T.; Wieghardt, K. *Inorg. Chem.* **2008**, *47*, 10935. (h) Ghosh, M.; Sproules, S.; Weyhermüller, T.; Wieghardt, K. *Inorg. Chem.* **2008**, *47*, 5963. (i) Muresan, N.; Lu, C. C.; Ghosh, M.; Peters, J. C.; Abe, M.; Henling, L. M.; Weyhermüller, T.; Bill, E.; Wieghardt, K. *Inorg. Chem.* **2008**, *47*, 4579. (j) Lu, C. C.; Bill, E.; Weyhermüller, T.; Bothe, E.; Wieghardt, K. *J. Am. Chem. Soc.* **2008**, *130*, 3181. (k) Ghosh, M.; Weyhermüller, T.; Wieghardt, K. *Dalton Trans.* **2008**, 5149. (l) Muresan, N.; Weyhermüller, T.; Wieghardt, K. *Dalton Trans.* **2007**, 4390. (m) Lu, C. C.; Bill, E.; Weyhermüller, T.; Bothe, E.; Wieghardt, K. *Inorg. Chem.* **2007**, *46*, 7880. (n) Kapre, R. R.; Bothe, E.; Weyhermüller, T.; George, S. D.; Muresan, N.; Wieghardt, K. *Inorg. Chem.* **2007**, *46*, 7827. (o) Muresan, N.; Chiopek, K.; Weyhermüller, T.; Neese, F.; Wieghardt, K. *Inorg. Chem.* **2007**, *46*, 5327. (p) Chlopek, K.; Bothe, E.; Neese, F.; Weyhermüller, T.; Wieghardt, K. *Inorg. Chem.* **2006**, *45*, 6298. (q) Chlopek, K.; Bill, E.; Weyhermüller, T.; Wieghardt, K. *Inorg. Chem.* **2005**, *44*, 7087. (r) Kokatam, S.; Weyhermüller, T.; Bothe, E.; Chaudhuri, P.; Wieghardt, K. *Inorg. Chem.* **2005**, *44*, 3709. (s) Bianchard, S.; Bill, E.; Weyhermüller, T.; Wieghardt, K. *Inorg. Chem.* **2004**, *43*, 2324. (t) Chun, H.; Bill, E.; Weyhermüller, T.; Wieghardt, K. *Inorg. Chem.* **2002**, *41*, 5091. (u) Chun, H.; Chaudhuri, P.; Weyhermüller, T.; Wieghardt, K. *Inorg. Chem.* **2002**, *41*, 790. (v) Chun, H.; Verani, C. N.; Chaudhuri, P.; Bothe, E.; Bill, E.; Weyhermüller, T.; Wieghardt, K. *Inorg. Chem.* **2001**, *40*, 4157. (w) Chaudhuri, P.; Verani, C. N.; Bill, E.; Bothe, E.; Weyhermüller, T.; Wieghardt, K. *J. Am. Chem. Soc.* **2001**, *123*, 2213. (6) (a) Brand, H.; Arnold, J. *Angew. Chem., Int. Ed.* **1994**, *33*, 95. (b) Stanciu, C.; Jones, M. E.; Fanwick, P. E.; Abu-Omar, M. M. *J. Am. Chem. Soc.* **2007**, *129*, 12400. (c) Blackmore, K. J.; Ziller, J. W.; Heyduk, A. F. *Inorg. Chem.* **2005**, *44*, 5559. (d) Haneline, M. R.; Heyduk, A. F. *J. Am. Chem. Soc.* **2006**, *128*, 8410. (e) Ketterer, N. A.; Fan, H.; Blackmore, K. J.; Yang, X.; Ziller, J. W.; Baik, M.-H.; Heyduk, A. F. *J. Am. Chem. Soc.* **2008**, *130*, 4364. (f) Blackmore, K. J.; Lal, N.; Ziller, J. W.; Heyduk, A. F. *J. Am. Chem. Soc.* **2008**, *130*, 2728. (g) Blackmore, K. J.; Sly, M. B.; Haneline, M. R.; Ziller, J. W.; Heyduk, A. F. *Inorg. Chem.* **2008**, *47*, 10522. (h) Zarkesh, R. A.; Ziller, J. W.; Heyduk, A. F. *Angew. Chem., Int. Ed.* **2008**, *47*, 4715. (i) Nguyen, A. I.; Blackmore, K. J.; Carter, S. M.; Zarkesh, R. A.; Heyduk, A. F. *J. Am. Chem. Soc.* **2009**, *131*, 3307. (j) Zarkesh, R. A.; Heyduk, A. F. *Organometallics* **2009**, *28*, 6629. (k) Szigethy, G.; Heyduk, A. F. *Inorg. Chem.* **2011**, *50*, 125. (l) Nguyen, A. I.; Zarkesh, R. A.; Lacy, D. C.; Thorson, M. K.; Heyduk, A. F. *Chem. Sci.* **2011**, *2*, 166. (7) (a) van Koten, G.; Vrieze, K. *Adv. Organomet. Chem.* **1982**, *21*, 151. (b) Vrieze, K. J. *Organomet. Chem.* **1986**, *300*, 307. (c) Mealli, C.; Ienco, A.; Phillips, A. D.; Galindo, A. *Eur. J. Inorg. Chem.* **2007**, 2556. (8) (a) Bart, S. C.; Hawrelak, E. J.; Lobkovsky, E.; Chirik, P. J. *Organometallics* **2005**, *24*, 5518. (b) Kreisel, K. A.; Yap, G. P. A.; Theopold, K. H. *Inorg. Chem.* **2008**, *47*, 5293. (9) (a) Richter, B.; Scholz, J.; Sieler, J.; Thiele, K.-H. *Angew. Chem., Int. Ed.* **1995**, *34*, 2649. (b) Spaniel, T.; Gorus, H.; Scholz, J. *Angew. Chem., Int. Ed.* **1998**, *37*, 1862. (c) Daff, P. J.; Etienne, M.; Donnadieu, B.; Knottenbelt, S. Z.; McGrady, J. E. *J. Am. Chem. Soc.* **2002**, *124*, 3818. (d) Scholz, J.; Gorus, H. *Polyhedron* **2002**, *21*, 305. (10) Arteaga-Müller, R.; Tsurugi, H.; Saito, T.; Yanagawa, M.; Oda, S.; Mashima, K. *J. Am. Chem. Soc.* **2009**, *131*, 5370.

- (11) Laguerre, M.; Dunogues, J.; Calas, R.; Duffaut, N. *J. Organomet. Chem.* **1976**, *112*, 49.
- (12) (a) Dieck, H.; Svoboda, M.; Greiser, T. Z. *Naturforsch. B* **1981**, *36*, 823. (b) van Asselt, R.; Elsevier, C. J.; Smeets, W. J. J.; Spek, A. L.; Benedix, R. *Recl. Trav. Chim. Pays-Bas* **1994**, *113*, 88.
- (13) Pangborn, A. B.; Giardello, M. A.; Grubbs, R. H.; Rosen, R. K.; Timmers, F. J. *Organometallics* **1996**, *15*, 1518.
- (14) Sheldrich, G. M. *Acta Crystallogr.* **2008**, *A64*, 112–122.
- (15) Altomare, A.; Burla, M. C.; Camalli, M.; Cascarano, G. L.; Giacovazzo, C.; Guagliardi, A.; Polidori, G. *J. Appl. Crystallogr.* **1994**, *27*, 435.
- (16) Farrugia, L. J. *J. Appl. Crystallogr.* **1999**, *32*, 837.
- (17) (a) Kawaguchi, H.; Yamamoto, Y.; Asaoka, K.; Tatsumi, K. *Organometallics* **1998**, *17*, 4380. (b) Mashima, K.; Matsuo, Y.; Tani, K. *Organometallics* **1999**, *18*, 1471. (c) Sanchez-Nieves, J.; Royo, P.; Pellinghelli, M. A.; Tiripicchio, A. *Organometallics* **2000**, *19*, 3161. (d) Nakamura, A.; Mashima, K. *J. Organomet. Chem.* **2001**, *621*, 224. (e) Tsurugi, H.; Ohno, T.; Yamagata, T.; Mashima, K. *Organometallics* **2006**, *25*, 3179. (f) Tsurugi, H.; Ohno, T.; Kanayama, T.; Arteaga-Müller, R.; Mashima, K. *Organometallics* **2009**, *28*, 1950.
- (18) Discussion of the coordination mode of folded ene-diamido chelates in d⁸ metal complexes: (a) Galindo, A.; Ienco, A.; Mealli, C. *New J. Chem.* **2000**, *24*, 73. (b) Galindo, A.; Gómez, M.; del Río, D.; Sánchez, F. *Eur. J. Inorg. Chem.* **2002**, 1326. (c) del Río, D.; Galindo, A. *J. Organomet. Chem.* **2002**, *655*, 16. (d) Galindo, A.; del Río, D.; Mealli, C.; Ienco, A.; Bo, C. *J. Organomet. Chem.* **2004**, *689*, 2847. (e) Wang, S.-Y. S.; Abboud, K. A.; Boncella, J. M. *J. Am. Chem. Soc.* **1997**, *119*, 11990. (f) Cameron, T. M.; Abboud, K. A.; Boncella, J. M. *Chem. Commun.* **2001**, 1224. (g) Cameron, T. M.; Ortiz, C. G.; Ghiviriga, I.; Abboud, K. A.; Boncella, J. M. *Organometallics* **2001**, *20*, 2032. (h) Cameron, T. M.; Ghiviriga, I.; Abboud, E. A.; Boncella, J. M. *Organometallics* **2001**, *20*, 4378. (i) Ison, E. A.; Cameron, T. M.; Abboud, K. A.; Boncella, J. M. *Organometallics* **2004**, *23*, 4070. (j) Hayton, T. W.; Boncella, J. M.; Scott, B. L.; Abboud, K. A.; Mills, R. C. *Inorg. Chem.* **2005**, *44*, 9506.
- (19) See the Supporting Information for the molecular structure of the cationic part of **3c**.
- (20) Kaupp, M.; Stoll, H.; Preuss, H.; Kaim, W.; Stahl, T.; van Koten, G.; Wissing, E.; Smeets, W. J. J.; Spek, A. L. *J. Am. Chem. Soc.* **1991**, *113*, S606.
- (21) (a) Poli, R. *Angew. Chem., Int. Ed.* **2006**, *45*, S058. (b) Debuigne, A.; Poli, R.; Jérôme, C.; Jérôme, R.; Detrembleur, C. *Prog. Polym. Sci.* **2009**, *34*, 211. (c) Wayland, B. B.; Poszmik, G.; Mukerjee, S. L.; Fryd, M. *J. Am. Chem. Soc.* **1994**, *116*, 7943. (d) Grogne, E. L.; Claverie, J.; Poli, R. *J. Am. Chem. Soc.* **2001**, *123*, 9513. (e) Stoffelbach, F.; Poli, R.; Richard, P. J. *Organomet. Chem.* **2002**, *663*, 269. (f) Shaver, M. P.; Allan, L. E. N.; Gibson, V. C. *Organometallics* **2007**, *26*, 4725. (g) Allan, L. E. N.; Shaver, M. P.; White, A. J. P.; Gibson, V. C. *Inorg. Chem.* **2007**, *46*, 8963. (h) MacLeod, K. C.; Conway, J. L.; Tang, L.; Smith, J. J.; Corcoran, L. D.; Ballem, K. H. D.; Patrick, B. O.; Smith, K. M. *Organometallics* **2009**, *28*, 6798. (i) MacLeod, K. C.; Conway, J. L.; Patrick, B. O.; Smith, K. M. *J. Am. Chem. Soc.* **2010**, *132*, 17325. (j) Champouret, Y.; MacLeod, K. C.; Baisch, U.; Patrick, B. O.; Smith, K. M.; Poli, R. *Organometallics* **2010**, *29*, 167. (k) Champouret, Y.; MacLeod, K. C.; Smith, K. M.; Patrick, B. O.; Poli, R. *Organometallics* **2010**, *29*, 3125. (l) Shaver, M. P.; Hanhan, M. E.; Jones, M. R. *Chem. Commun.* **2010**, 46, 2127. (m) Zhou, W.; Tang, L.; Patrick, B. O.; Smith, K. M. *Organometallics* **2011**, *30*, 603. (n) Allan, L. E. N.; Cross, E. D.; Francis-Pranger, T. W.; Hanhan, M. E.; Jones, M. R.; Pearson, J. K.; Perry, M. R.; Storr, T.; Shaver, M. P. *Macromolecules* **2011**, *44*, 4072.
- (22) (a) Tsarevsky, N. V.; Matyjaszewski, K. *Chem. Rev.* **2007**, *107*, 2270. (b) Pintauer, T.; Matyjaszewski, K. *Chem. Soc. Rev.* **2008**, *37*, 1087. (c) Ouchi, M.; Terashima, T.; Sawamoto, M. *Chem. Rev.* **2009**, *109*, 4963. (d) Satoh, K.; Kamigaito, M. *Chem. Rev.* **2009**, *109*, 5120. (e) Rosen, B. M.; Percec, V. *Chem. Rev.* **2009**, *109*, 5069 and references therein.
- (23) We monitored the reaction of **2a**/CCl₄ and **2a**/PhCH₂Br by UV-vis spectra, and the activation of Cl-CCl₃ was much faster than that of Br-CH₂Ph. Changes of the UV-vis spectra for **2a**/PhCH₂Br are shown in Figure S9 in Supporting Information.
- (24) (a) Kotani, Y.; Kamigaito, M.; Sawamoto, M. *Macromolecules* **1999**, *32*, 2420. (b) Stoffelbach, F.; Haddleton, D. M.; Poli, R. *Eur. Polym. J.* **2003**, *39*, 2099.
- (25) (a) Asandei, A. D.; Moran, I. W. *J. Am. Chem. Soc.* **2004**, *126*, 15932. (b) Asandei, A. D.; Chen, Y. *Macromolecules* **2006**, *39*, 7549.
- (26) (a) Mashima, K.; Ohnishi, R.; Yamagata, T.; Tsurugi, H. *Chem. Lett.* **2007**, *36*, 1420. (b) De Waele, P.; Jazdzewski, B. A.; Klosin, J.; Murray, R. E.; Theriault, C. N.; Vosejka, P. C.; Petersen, J. L. *Organometallics* **2007**, *26*, 3896. (c) Tsurugi, H.; Ohnishi, R.; Kaneko, H.; Panda, T. K.; Mashima, K. *Organometallics* **2009**, *28*, 680.
- (27) For the comparison of the reactivity of trichloromethyl- and benzyl-radicals, we examined the reaction of **2b** with benzyl bromide in the presence of excess styrene. Incorporation of styrene was not observed when benzyl bromide was used, and the benzyl radical attacked the ligand to form (PhCH₂-amido-imino)TaCl₄, indicating that recombination of benzylic radical and ligand-based radical was much faster than that of trichloromethyl-based and ligand-based radical due to the stability of trichloromethyl radical compared with benzylic radical toward radical recombination (see Scheme S1 in Supporting Information).
- (28) (a) Chao, Y.-W.; Wexler, P. A.; Wigley, D. E. *Inorg. Chem.* **1989**, *28*, 3860. (b) Suh, S.; Hoffman, D. M. *Inorg. Chem.* **1996**, *35*, 5015. (c) Guérin, F.; McConville, D. H.; Vittal, J. J.; Yap, G. A. P. *Organometallics* **1998**, *17*, 1290. (d) Araujo, J. P.; Wicht, D. K.; Bonitatebus, P. J.; Schrock, R. R. *Organometallics* **2001**, *20*, 5682. (e) Oshiki, T.; Tanaka, K.; Yamada, J.; Ishiyama, T.; Kataoka, Y.; Mashima, K.; Tani, K.; Takai, K. *Organometallics* **2003**, *22*, 464. (f) Oshiki, T.; Yamada, A.; Kawai, K.; Arimitsu, H.; Takai, K. *Organometallics* **2007**, *26*, 173.
- (29) (a) Cope-Eatough, E. K.; Mair, F. S.; Pritchard, R. G.; Warren, J. E.; Woods, R. J. *Polyhedron* **2003**, *22*, 1447. (b) Laine, T. V.; Klinga, M.; Maaninen, A.; Aitola, E.; Leskela, M. *Acta Chem. Scand.* **1999**, *53*, 968. (c) El-Ayaan, U.; Paulovicova, A.; Fukuda, Y. *J. Mol. Struct.* **2003**, *645*, 205.
- (30) (a) Recknagel, A.; Noltemeyer, M.; Edelman, F. T. *J. Organomet. Chem.* **1991**, *410*, 53. (b) Bochkarev, M. N.; Trifonov, A. A.; Cloke, F. G. N.; Dalby, C. I.; Matsunaga, P. T.; Andersen, R. A.; Schumann, H.; Loebel, J.; Hemling, H. *J. Organomet. Chem.* **1995**, *486*, 177. (c) Scholz, A.; Thiele, K.-H.; Scholz, J.; Weimann, R. *J. Organomet. Chem.* **1995**, *501*, 195. (d) Trifonov, A. A.; Kirillov, E. N.; Bochkarev, M. N.; Schumann, H.; Muehle, S. *Russ. Chem. Bull.* **1999**, *48*, 382. (e) Trifonov, A. A.; Kurskii, Y. A.; Bochkarev, M. N.; Muehle, S.; Dechert, S.; Schumann, H. *Russ. Chem. Bull.* **2003**, *52*, 601. (f) Trifonov, A. A.; Fedorova, E. A.; Ikskii, V. N.; Dechert, S.; Schumann, H.; Bochkarev, M. N. *Eur. J. Inorg. Chem.* **2005**, 2812. (g) Moore, J. A.; Cowley, A. H.; Gordon, J. C. *Organometallics* **2006**, *25*, 5207. (h) Walter, M. D.; Berg, D. J.; Andersen, R. A. *Organometallics* **2007**, *26*, 2296. (i) Cui, P.; Chen, Y.; Wang, G.; Li, G.; Xia, W. *Organometallics* **2008**, *27*, 4013. (j) Panda, T. K.; Kaneko, H.; Pal, K.; Tsurugi, H.; Mashima, K. *Organometallics* **2010**, *29*, 2610.
- (31) Labauze, G.; Samuel, E.; Livage, J. *Inorg. Chem.* **1980**, *19*, 1384.
- (32) Cloke, F. G. N.; Dix, A. N.; Green, J. C.; Perutz, R. N.; Seddon, E. A. *Organometallics* **1983**, *2*, 1150.
- (33) Noh, W.; Girolami, G. S. *Inorg. Chem.* **2008**, *47*, 535.
- (34) (a) Richter, S.; Daul, C.; Aelwsky, A. V. *Inorg. Chem.* **1976**, *15*, 943. (b) Gardiner, M. G.; Hanson, G. R.; Henderson, M. J.; Lee, F. C.; Raston, C. L. *Inorg. Chem.* **1994**, *33*, 2456. (c) Rijnberg, E.; Boersma, J.; Jastrzebski, J. T. B. H.; Lakin, M. T.; Spek, A. L.; van Koten, G. *Organometallics* **1997**, *16*, 3158. (d) Rijnberg, E.; Richter, B.; Thiele, K.-H.; Boersma, J.; Veldman, N.; Spek, A. L.; van Koten, G. *Inorg. Chem.* **1998**, *37*, 56.
- (35) See Supporting Information.
- (36) In the EPR spectra of **8b** and **8c** in THF, the resonances for tantalum-centered radical became larger than those observed in toluene or CH₂Cl₂ (Figures S15 and S16 in Supporting Information). The equilibrium between metal and ligand-centered radical character was probably affected by the coordinating solvent. In addition, the increase of the intensity for signals of the ligand-centered radical was observed with increasing the temperature (Figure S17 in Supporting

Information), suggesting the equilibrium of the two redox isomers was affected by the solvent and temperature.

(37) Absorption band at 400 nm corresponds to cobaltocene cation: Warratz, R.; Peters, G.; Studt, F.; Römer, R.-H.; Tuczek, F. *Inorg. Chem.* **2006**, *45*, 2531.

(38) Consumption of **8b** was monitored by the EPR measurement to check the disappearance of both resonances during the reduction: controlled amount of Cp₂Co (0.75 equiv) was added to the toluene solution of **8b**, and both resonances were weakened (Figure S19 in Supporting Information). By the addition of 1 equiv of Cp₂Co, the reaction solution was EPR silent and the complex **9b** was detected in the ¹H NMR spectrum.

(39) (a) Ue, M.; Takeda, M.; Takehara, M.; Mori, S. *J. Electrochem. Soc.* **1997**, *144*, 2684. (b) Shundrin, L. A.; Bardin, V. V.; Frohn, H.-J. *Z. Anorg. Allg. Chem.* **2004**, *630*, 1253. (c) Sorin, G.; Mallorquin, R. M.; Contie, Y.; Baralle, A.; Malacria, M.; Goddard, J.-P.; Fensterbank, L. *Angew. Chem., Int. Ed.* **2010**, *49*, 8721.

(40) When NaBF₄ was used instead of NaBPh₄, reduction of the ligand was not observed.

(41) In the case of the reaction of **8b** with AIBN at 60 °C for 60 h, the AIBN-derived radical attacked to the ligand backbone to form a new tantalum complex as the main product together with unidentified tantalum species (Scheme S2 in Supporting Information). Reaction details are shown in Supporting Information.